Accepted Manuscript

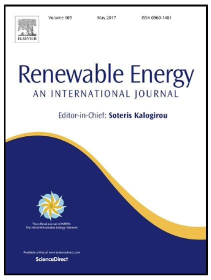

Power-to-gas and power-to-liquid for managing renewable electricity intermittency in the Alpine Region

Sennai Mesfun, Daniel L. Sanchez, Sylvain Leduc, Elisabeth Wetterlund, Joakim Lundgren, Markus Biberacher, Florian Kraxner

PII:	S0960-1481(17)30098-8
DOI:	10.1016/j.renene.2017.02.020
Reference:	RENE 8527
To appear in:	*Renewable Energy*
Received Date:	09 August 2016
Revised Date:	06 February 2017
Accepted Date:	07 February 2017

Please cite this article as: Sennai Mesfun, Daniel L. Sanchez, Sylvain Leduc, Elisabeth Wetterlund, Joakim Lundgren, Markus Biberacher, Florian Kraxner, Power-to-gas and power-to-liquid for managing renewable electricity intermittency in the Alpine Region, *Renewable Energy* (2017), doi: 10.1016/j.renene.2017.02.020

Highlights:

- BeWhere, a MILP optimization model, simulates energy systems in the Alpine Region.
- Power-to-gas and power-to-liquid enable large scale integration of renewables.
- Power-to-gas and power-to-liquid allow decarbonizing diverse CO_2–emitting sectors.
- Scenarios pertaining to the impact of carbon policy and fossil prices investigated.

Power-to-gas and power-to-liquid for managing renewable electricity intermittency in the Alpine Region

Sennai Mesfun[1,2,*], Daniel L. Sanchez[3], Sylvain Leduc[2], Elisabeth Wetterlund[1,2], Joakim Lundgren[1,2], Markus Biberacher[4], Florian Kraxner[2]

[1]Luleå University of Technology, Energy Engineering, Division of Energy Science, SE-971 87 Luleå, Sweden

[2]International Institute for Applied Systems Analysis (IIASA), Schlossplatz 1, A-2361 Laxenburg, Austria

[3]Carnegie Institution for Science, Department of Global Ecology, 260 Panama St., Stanford, CA 94305

[4]Research Studios Austria (RSA), Studio iSPACE, Schillerstrasse 25, A-5020 Salzburg, Austria

Abstract:

Large-scale deployment of renewable energy sources (RES) plays a central role in reducing CO_2 emissions from energy supply systems, but intermittency from solar and wind technologies presents integration challenges. High temperature co-electrolysis of steam and CO_2 in power-to-gas (PtG) and power-to-liquid (PtL) configurations could utilize excess intermittent electricity by converting it into chemical fuels. These can then be directly consumed in other sectors, such as transportation and heating, or used as power storage. Here, we investigate the impact of carbon policy and fossil fuel prices on the economic and engineering potential of PtG and PtL systems as storage for intermittent renewable electricity and as a source of low-carbon heating and transportation energy in the Alpine region. We employ a spatially and temporally explicit optimization approach of RES, PtG, PtL and fossil technologies in the electricity, heating, and transportation sectors, using the BeWhere model. Results indicate that large-scale deployment of PtG and PtL technologies for producing chemical fuels from excess intermittent electricity is feasible, particularly when incentivized by carbon prices. Depending on carbon and fossil fuel price, 0.15−15 million tonnes/year of captured CO_2 can be used in the synthesis of the chemical fuels, displacing up to 11% of current fossil fuel use in transportation. By providing a physical link between the

*Corresponding author. Tel.: +43(0) 2236 807 661.
Email address: mesfun@iiasa.ac.at (S. Mesfun).

electricity, transportation, and heating sectors, PtG and PtL technologies can enable greater integration of RES into the energy supply chain globally.

Keywords: Renewable energy; power-to-gas; power-to-liquid; energy systems optimization; spatial and temporal modelling.

1. Introduction

In order to mitigate climate change and reduce GHG emissions, several technologies are being developed and deployed. Notably, carbon capture and sequestration (CCS) is being developed as a post-combustion remedy for fossil fuel based energy processes [1], and for bio-energy processes (in the so-called BECCS configuration) in the context of negative emissions [2–4]. Other mitigation techniques include substitution of fossil fuels with carbon-free or low-carbon energy technologies (such as solar, wind, geothermal, hydro, biomass etc.). Decarbonization of the energy sector by increasing the share of renewables is an essential step towards the deployment of low-carbon and sustainable energy systems. However, power generated from renewable energy sources (RES), in particular from solar and wind, is affected by the intermittency of resources. In addition to intermittency, the temporal and spatial mismatch between availability of resources (wind and insolation) and energy demand (consumers) creates further challenges. As a result, large-scale deployment of solar and wind technologies could impact the reliability of power systems. Large-scale storage systems, such as batteries, compressed-air, flywheel and pumped-hydro, could help even out this supply-demand mismatch. Moreover, most RES produce electricity, which means that they can either displace fossil fuel usage in the electricity sector or power electrified transportation vehicles. This could limit the role of most RES in economy-wide decarbonization of energy supply systems, which emit CO_2 from a wide range of sources outside of the electricity sector.

The main focus of this work is to examine the impacts of temporal and spatial intermittency of RES on power dispatch systems and how excess intermittent electricity can be captured via power-to-gas and power-to-liquid (PtG and PtL) processes for use in other energy sectors (such as transportation and heating). In this regard, the PtG and PtL technologies can offer benefits that would make it a useful addition to conventional storage technologies.

Here, we investigate the impact of carbon policy and fossil fuel prices on the economic and engineering potential of PtG and PtL systems as storage for intermittent renewable electricity and as a source of low-carbon heating and transportation energy in the Alpine region. The Alpine region is a pertinent study region as it has the potential for diverse RES generation, including biomass, solar, wind and hydropower, and is subject to the European Union's CO_2 emissions regulations. Despite several reports examining the role PtG and/or PtL might play in low-carbon energy systems (e.g., [5–9]), to the knowledge of the authors no prior work has used high-resolution energy planning models to assess PtG and PtL deployment. Prior analyses of PtG and PtL deployment typically assume a fixed level of RES integration (e.g., [6,10,11]) or evaluate these technologies using a techno-economic assessment, rather than systems analysis. In contrast, we evaluate PtG and PtL technologies using a high-resolution decision support model on a regional level. Specifically, we employ a spatially and temporally explicit optimization of RES, PtG, PtL, and fossil technologies in the electricity, heating, and transportation sectors. This work has broad relevance to efforts to introduce more renewable energy into the electricity sector, and the deep decarbonization of energy systems.

2. Power-to-gas and Power-to-liquid configurations

As discussed in the introduction, PtG could play a central role in enabling intermittent renewables to have a greater share of energy supply. Intermittent renewables generate electricity, and PtG and PtL processes can allow RES to produce fuels for other sectors such as transportation and heating. Figure 1 illustrates the power balancing and long-term storage concepts investigated in this paper. In this process, the energy over-generated from the power system can be stored in gas/liquid fuels via electrochemical reduction of gas-phase H_2O and CO_2. The reduced gas, similar in composition to synthetic gas (otherwise known as syngas), can then be used for the synthesis of higher-quality transportation/gas fuels.

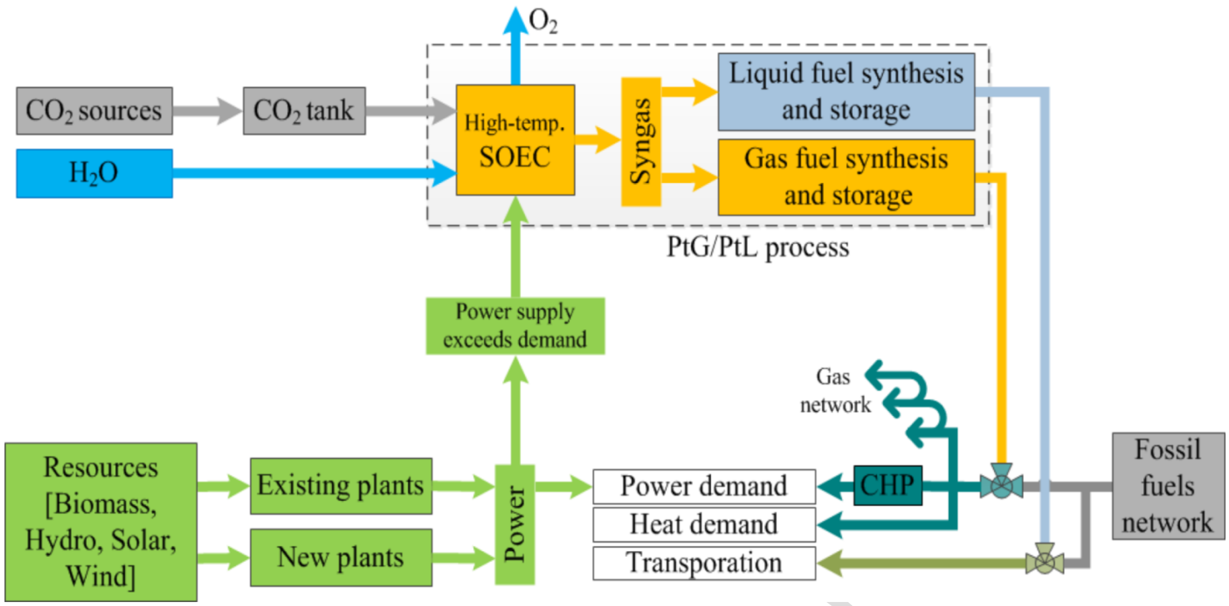

Figure 1. *Schematics of the power balancing and long-term storage concept PtG and PtL, which can enhance renewable energy integration via use of excess intermittent electricity in the heating, transportation and power sectors.*

2.1. Solid-oxide electrolysis cell

Electrolysis is central to the PtG and PtL concepts. Electrolysis is an electrochemical process in which a direct electric current is passed between two electrodes through an ionized medium (an electrolyte) to deposit positively and negatively charged ions onto their respective electrodes. Electrolyzers can be broadly classified into low- and high-temperature processes with conversion efficiencies ranging from 60 to 80% of electricity stored as chemical energy in hydrogen or syngas [8,11,12].

High-temperature solid oxide electrolysis cells (SOECs) are gaining interest, as they can be operated at temperatures in the range of 700–1000°C, meaning that part of the energy required to electrochemically dissociate H_2O (in the case of water electrolysis) or H_2O(g) and CO_2 (in the case of co-electrolysis) is supplied as heat energy, thereby minimizing energy input in the form of electricity [13]. Thus, the performance of high-temperature SOECs has the advantage of both thermodynamic efficiency and faster reaction rates [14,15]. The heat required can be externally supplied via heat exchangers in the case of a low current density operation, or it can be internally generated using the inevitable ohmic cell resistance when the SOEC is operated at high current densities in order to maintain adequate production rates of H_2 or syngas.

In this context, the high-temperature co-electrolysis of steam and CO_2 (e.g., [13,16–24]) using SOECs can offer an attractive option for converting excess electricity into liquid/gas fuels that can be directly used in the transportation, heating or power sectors. Co-electrolysis adds flexibility to the energy supply chain by creating links among the different energy sectors. Furthermore, it allows large volumes of CO_2 to be recycled, which can play a significant role in decarbonizing the energy supply system.

The co-electrolysis characteristic of SOECs is of substantial importance here. This is because co-electrolysis generates products that can be readily upgraded into liquid/gas fuels with existing market infrastructure in a one-step process. In principle, syngas can be produced in a two-step process, electrolysis of H_2O to produce H_2 followed by conversion of H_2-CO_2 into syngas through a reverse shift water-gas reaction. In subsequent stages the syngas is catalytically upgraded into methane (the Sabatier process) or higher grade hydrocarbons [8,13]. In contrast, the co-electrolysis process reduces the process steps by directly depositing high quality syngas (mainly H_2 and CO) on the cathode via simultaneous electrochemical reduction of H_2O and CO_2. In so doing, the gas deposited on the anode is pure O_2, which could also bring additional value to the process. In this study, however, no revenue is considered from O_2. Furthermore, the operation mode of SOECs can be altered to produce different types of syngas, for instance, by controlling the composition of the feed stream to the SOECs the quality of the syngas can be tailored to enhance catalytic conversion into synthetic fuels at later stages [14].

Recent development and performance improvements have demonstrated efficient co-electrolysis of H_2O(g) and CO_2 in SOECs. The ohmic resistance as well as the cell degradation rates and mechanisms are similar, as in the electrolysis of steam alone [17,21]. In the light of such SOEC developments, an overall conversion efficiency of 70% for PtL (the ratio of the calorific value of the liquid fuel produced, such as methanol, to power input) [6,25] and 80% for PtG (the ratio of the calorific value of methane produced to power input) [26] are possible. Unless stated otherwise, in this work an overall efficiency of 70% is assumed for both PtG and PtL technologies. This efficiency refers to the calorific value of the final product (liquid methanol in the case of PtL and methane gas in the case of PtG) and the power input to the process.

3. BeWhere Alps model

We use the BeWhere model, initially developed by IIASA and the Luleå University of Technology. BeWhere is a geographically explicit cost optimization model employing mixed integer linear programming (MILP), written in the General Algebraic Modeling System (GAMS) and using CPLEX as a solver. Earlier applications of the model were focused on planning and localization of bioenergy systems. So far, several researchers have demonstrated its application under different contexts. These include, for instance, methanol via biomass gasification [27–29], second generation biofuels on a EU scale [30,31], cost-effective CO_2 emission reduction through bioenergy [32,33], and polygeneration in different locations [34–37].

The BeWhere Alps model is an enhanced version which includes other forms of RES in addition to biomass, namely solar, wind and hydropower. This work particularly focuses on the application of BeWhere to investigate the impact of carbon and fossil fuel prices, as well as the impact of temporal and spatial intermittency of RES, when planning coordinated decarbonization of the energy supply system in the Alpine Region.

3.1. Set-up of the optimization model

The overall objective is to minimize the total cost of the complete energy supply chain including the cost of CO_2 emissions, according to the following expression:

$$\min f = \sum_{c} (\text{cost}_c^{\text{supply chain}} + \text{emissions}_c^{CO_2} \times \text{cost}_c^{CO_2}) \quad (1)$$

The model satisfies different sets of constraints in relation to power generation mix: those that ensure the power demand is met at all hours in all the regions; those that ensure the share of fossil-based power is generated within the country in which it is used; and those that ensure prioritization of RES-based power use. The first set of constraints satisfies power demand using the least expensive options based on generation and existing transmission availability. The second set of constraints prevents transmission of fossil-based power (from baseload coal and dispatchable natural gas plants). The third set of constraints prioritizes the use of RES-based power generation; that is, investment in RES only starts when it becomes feasible to directly satisfy power demand.

The optimization procedure considers the transmission to be a direct power flow balance. There is no attempt to mimic the voltage phase shift, which is highly nonlinear. However, the power flow balance approximation is a reasonable representation for a high-voltage direct-current (HVDC) transmission network [38]. The use of an HVDC transmission instead of high-voltage alternating-current (HVAC) is because of the nonlinear nature of HVAC, which significantly complicates the optimization. However, the HVDC transmission can be thought of as an approximation of HVAC in terms of power flow because it includes electrical losses and describes transmission at a high level.

The objective function, (1), accounts for the total cost of generation, transmission and storage of an electric power system for a selected time frame. It is assumed that there is only one type of dispatchable generator (natural gas combined cycle) as the aim is to consider a high penetration- level and variable-generation system. Cost optimization is superior to a load-matching optimization for real world applications, as cost is a primary driver of incorporation of variable generation into an electric power system.

Weather data are used for estimating the wind and solar photovoltaic (PV) power outputs, as discussed further in Sections 3.4.3. and 3.4.4. The natural gas plants are assumed to be back-up energy generation for when RES-based power cannot meet electrical demand. Our basic approach is to take the salient variables (wind speed, solar irradiance, etc.) from a numerical weather prediction model and process them through a model that mimics the behavior of a wind turbine and solar PV panels. The output takes into account the engineering constraints of the technologies as well as weather.

3.2. Carbon pricing and fossil fuel market scenarios

Carbon pricing plays central role in enabling greater share of renewables in the energy system. In this work, the BeWhere model is used to investigate the influence of carbon policy (CO_2 prices) and fossil fuel prices on the mix of energy supply. Fossil fuel prices often introduce a large degree of uncertainty into long-term planning of energy systems, while policies regarding CO_2 emissions vary greatly among countries. Our approach encompasses this range of uncertainty through scenario analysis. With this in mind, the model is run over a range of 0–200 €/tonne of CO_2 at an interval of 50 €/tonne. In turn, each interval is evaluated for different fossil fuels prices (base case, medium, high). The base case is assumed at 100 €/tonne of CO_2 and current market prices for fossil fuels. Table 1 introduces the scenarios considered in this study.

Table 1. Scenario matrix for carbon pricing and fossil fuel market factors

		Carbon pricing factors				
	Scenario	zero	low	base-case	medium	high
Fossil fuel price factors (FFPs)	base-case	S{0, 1}[a]	S{0.5, 1}	S{1, 1}	S{1.5, 1}	S{2, 1}
	medium	S{0, 1.5}	S{0.5, 1.5}	S{1, 1.5}	S{1.5, 1.5}	S{2, 1.5}
	high	S{0, 2}	S{0.5, 2}	S{1, 2}	S{1.5, 2}	S{2, 2}

[a]Set of factors denote Scenario {Carbon pricing factor, FFPs}

S{1, 1} represents base case scenario, €100/tCO2 and market prices for fossil at the reference time.

S{1, 1.5} and S{1, 2} represent for base case carbon price and FFPs 50 and 100% higher than the current market prices, respectively.

S{1.5, 1} and S{2, 1} represent for base case FFPs and carbon prices 50 and 100 % higher than the base case, respectively.

S{1.5, 1.5}, S{1.5, 2}, S{2, 1.5} and S{2, 2} represent for scenarios where FFPs and carbon prices are 50 and 100% higher than their base case values, simultaneously and alternately. These price sets illustrate realistic future scenarios as FFPs and carbon price are intrinsically related parameters.

3.3. System boundaries and geographic resolution

The boundaries of the model are limited to the Alpine region, which includes parts of seven European nations, as shown in **Figure 2**. Liechtenstein is excluded from the analysis because of its small size. In the model, the entire Alpine region is divided into about 3,000 grid cells with a spatial resolution of 0.1 degree (approximately 10x10 km).

During the optimization process, each grid cell essentially represents demand area (in terms of heating and transportation), supply area (in terms of resource availability such as biomass, river catchment, insolation and wind) and potential locations for new power plant installation.

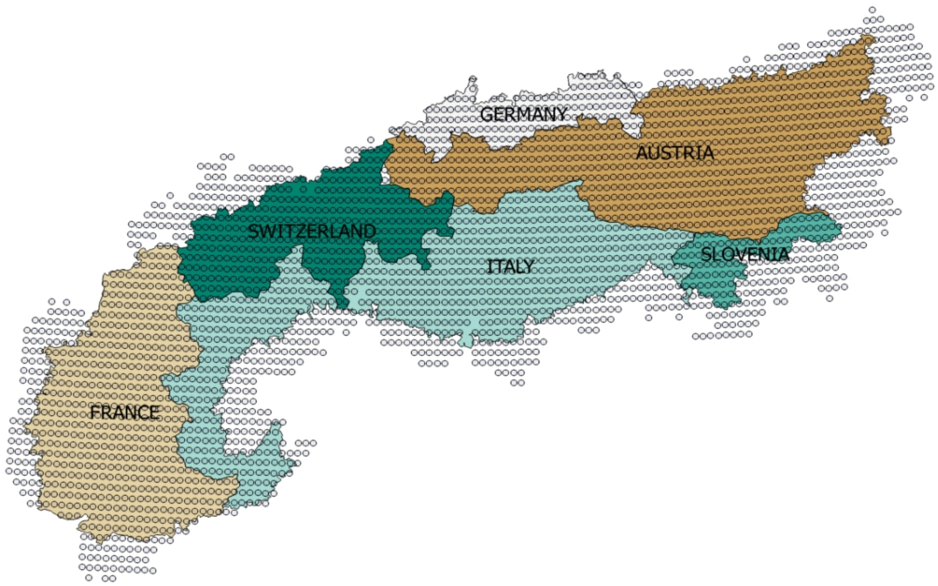

Figure 2. *The Alpine region by country and the spatial grid cells used for energy demand and supply.*

3.4. Supply chain

The energy supply chain considered in this study is comprised of different technologies and resources. The model includes biomass (for producing electricity, heat and biofuels), hydropower (existing plants and the potential for new installations), solar PV and wind. The data collection and processing methods for every resource considered are described in detail below. The costs of technologies are documented in Appendix A.

Common to all technologies are the different environmental protections in the Alpine Region, such as national parks and reserves, regional parks, United Nations Educational, Scientific and Cultural Organization (UNESCO) reserves and world heritage sites [39]. This limits resources and constrains facility locations. The different levels of protection are represented in the model according to their priority order (high, medium, low and no protection). Difficulties related to the harvesting of resources (e.g., biomass) and to the installation of power plants (e.g., combined heat and power plant (CHP), wind, solar and hydro) due to elevation and landscape profiles put further limitation on amount of energy that can be generated. As a result, locations beyond 2000 m in elevation (for a low environmental restriction scenario) and 1200 m (for a strict environmental protection scenario) are excluded from the analysis.

3.4.1 Bioenergy

Different biomass feedstocks (e.g., forest residue, agricultural residue) and conversion technologies (e.g., biomass steam turbines, combined heat and power, and integrated gasification combined cycle (bIGCC)) can be used for the production of bioenergy. In this work, the biomass feedstock refers to forest residue which is assumed to be converted into heat and power via bIGCC technology. Two bIGCC plant sizes with different heat-to-power output ratios are considered for biomass conversion. The details of the technologies and the associated costs are provided in Appendix A, Table A1.

The potential supply of biomass in each grid cell is estimated based on the share of net primary production that is forest and the annual increment of forest biomass. A brief description of the methodology can be found in [33,35,40]. Here, the annual biomass increment in each grid cell is explicitly introduced into the model. No distinction is made between different tree species. The available forest biomass is assumed to have a density of 500 kg/m^3 (dry weight), with a heating value of 18.5 GJ/tonne (lower heating value (LHV) of dry feedstock) and a moisture content of 55%. Hourly energy production estimates are obtained by averaging the annual potential over the total number of hours in a year.

In the model, forest residues can be transported to production plants in three ways: truck, train or boat. The data for the cost of transportation and related emissions used in the model are summarized in Appendix A, Table A2. The transportation cost is composed of fixed (to account for loading and unloading, independent of distance) and variable (to account for distance) cost components. A network map of roads and rails is used to estimate the distance between supply and production plants. Details on transport data processing can be found in [41].

3.4.2. Hydropower

Our representation of hydropower includes both existing capacities and the potential for new installations. Hydropower potential is estimated based on river catchment areas outside the protected regions of the Alps. Annual power production potentials are estimated based on river flow rates and mean head data acquired from [42]. In the model, hourly generation potential from hydropower is obtained by averaging the annual estimates over the total number of hours in a year. At this stage, seasonal variations in the amount of water are not considered. The costs assumed for new hydropower plants are documented in Appendix A, Table A3.

3.4.3. Solar energy

The hourly capacity factors and capacity limits for solar energy are derived from high-resolution global climate reconstruction data. Solar insolation data are collected from an open access database developed at Princeton University [43]. Hourly solar insolation estimates from the year 2010 are processed at a 3-hourly temporal resolution and a 0.25 degree spatial resolution.

In order to estimate solar power output from solar insolation, a conversion efficiency of 15% is assumed. Capacity factors for 2010 are taken as the ratio of derived power to maximum power output in the year 2010, for each hour in each grid cell. Capacity limits are taken as the maximum power output in 2010. Data are projected for a 0.1 degree spatial resolution in order to match with the resolution used in this work, based on the grid cell with the largest overlap. The solar capacity factors are sampled for the same hours as demand, which is described in a subsequent section. The costs associated with the solar PV technology considered in this work are reported in Appendix A, Table A3.

3.4.4. Wind energy

Like solar, the hourly capacity factors, and capacity limits, for wind energy are derived from the high-resolution global climate reconstruction data from Princeton University [43]. Hourly wind speed from the year 2010 is used. Wind speed estimates in areas with high surface roughness, like the Alps, are very uncertain. As such, derived capacity factors should be approached with caution.

The wind energy harvested per unit area which is swept by the turbine rotor is derived using the methodology of the Alpine windharvest Partnership Network [44]. To find the hourly energy output, a specific curve with maximum power of 450 W/m^2 at a rated cut-out speed is assumed, based on the Austrian Wind Potential Analysis [45]. In order to derive power output in each grid cell, the wind turbines are assumed to be spaced 11 lengths apart. Capacity factor, capacity limits, sampling and interpolation methods are identical to those used in deriving solar inputs. Likewise, the costs associated with the assumed wind energy technology are reported in Appendix A, Table A3.

3.4.5 Natural gas and coal plants representation

In the model, any deficit in power supply is assumed to be balanced with dispatchable natural gas plants that mimic actual plant operations through a set of regulating ramping constraints. The ramping constraints are implemented such that the aggregated output of the dispatchable natural gas plants in the Alps region reaches a maximum (90% of the demand in the region) or falls down to zero within 120 minutes. Furthermore, the fossil model includes a coal fired base-load to cover 10% of the demand in each country in the region.

Moreover, the costs associated with fossil fuel based energy use are accounted in terms of the market values of the energy carriers, as reported in Table B1. Carbon emission intensities of fossil-based energy use represent actual figures for all countries that make up the Alps as summarized in Table C1.

3.5. Energy demand in the Alpine Region

3.5.1. Power demand in 2010

The hourly power demand for each country in the Alpine region is derived from the European Network of Transmission System Operators for Electricity (ENTSO-E). ENTSO-E reports historical demand at the country level[†]. The year 2010 is chosen, which is consistent with the estimates of wind and solar resources within the Alpine Region.

The hourly demand profiles to the portion of each country within the Alpine Region are scaled based on the fraction of the population living in the Alps. This assumes that per capita hourly demand is constant within a country. When data is unavailable in a specific hour, the data from the previous hour is used, or the same hour in the previous day, depending on data availability.

To reduce computational complexity, the demand is sampled every three hours from the peak and median day in each month. This is consistent with sampling methods from previous high-resolution electricity sector planning models [46]. In total, 192 hours are sampled throughout the year 2010 (8

[†] Available at https://www.entsoe.eu/data/data-portal/consumption/Pages/default.aspx

hours/day, 2 days/month and 12 months/year). Figure 3 shows the profile of the power demand of the year 2010 for the sampled hours.

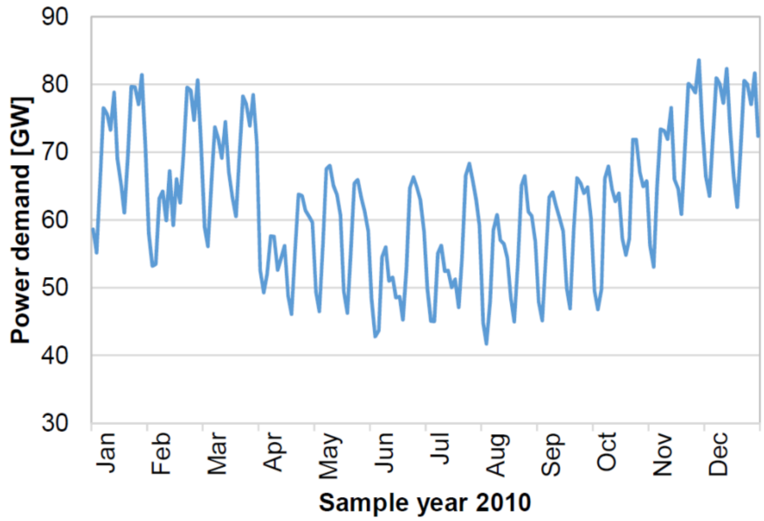

Figure 3. *Aggregated hourly power demand of the Alpine Region in 2010 at the sampled hours.*

To represent the entire year, the sampled days are weighted to represent multiple days by fixing peak days to represent one day of the month and median days to represent the remaining days in the month (i.e., days in a month minus one) [46,47]. Doing so ensures peak conditions are included in the power constraint while economic assessment is dominated by the typical demand profile, as peak demand occurrences are rare [47]. Accordingly, all samples (i.e. 8 samples per selected day) represent three hours each, peak days represent a day of the corresponding month and median days represent the remaining days in the month. This procedure is included in the model by means of a time-indexed weighting parameter.

3.5.2. District heating and transportation fuel demand

A distribution system for fossil, biofuels and gas/liquids is assumed to exist or be built within the demand areas. The demand in each area is estimated by introducing fuel consumption parameters for heating and transportation that are scaled by population. These parameters in turn refer to the fuel consumption data of the country to which the demand area belongs to. The data for carbon emission intensities in relation to fossil fuel use in the district heating and transportation sectors are summarized in Appendix C, Table C1.

Furthermore, the year is divided into three time periods of equal length so as to harmonize with seasonal variations in heating demand (e.g., [31]). Fuel demands per capita per unit time for heating and transportation for each country are summarized in Table 2.

Table 2. Heat (seasonal, denoted by *m*) and transport fuel demand data used in this study [31]

Country	Heat (GJ/capita/season)			Transport (GJ/capita/year)
	m_1	m_2	m_3	
Austria	12.1	1.7	0.8	16.4
France	49.0	26.0	6.7	114.6
Germany	163.3	86.6	22.4	192.2
Italy	16.3	2.4	1.1	67.1
Slovenia	39.4	5.7	2.7	69.5
Switzerland	13.4	7.1	1.8	40.5

3.6. CO_2 sources in the Alpine Region

Other than water, a significant portion of the feed stream to the high-temperature SOECs is CO_2. Preferably, CO_2 should be attained at low cost, high purity and flow rates large enough to match electricity over-generation from the power sector at any given time and location. Different sources can be identified as potential CO_2 providers. Commonly discussed sources include CO_2 from fossil power plants, CO_2 from biomass based CHPs and processes, CO_2 from other industrial processes and CO_2 from air. In this work, all types of power generation technologies that emit CO_2 within the Alpine Region are analyzed. No classification is made on plant type or on how the CO_2 is acquired. Direct air capture is excluded, as it is likely to be cost-prohibitive in the near-term [48].

Consequently, it is necessary to identify power plants that emit CO_2 in the Alpine Region. These locations are identified from the Carbon Monitoring for Action (CARMA) database [49] by overlapping a geographic map of the Alpine Region and a location map of CO_2 emitting industries in ArcGIS. A total of 136 potential CO_2 sources are identified within the region, see Figure 4. The CARMA database includes future projections for CO_2 emissions from the industrial sites, which is used in this work to constrain production capacities of PtG and PtL plants.

The identified CO_2 sources are potential locations for PtG and PtL plants. Fixing the location of PtG/PtL plant simplifies the optimization. Transmitting excess electricity from the power grid via existing transmission lines is likely easier than transporting CO_2 to locations along the power grid.

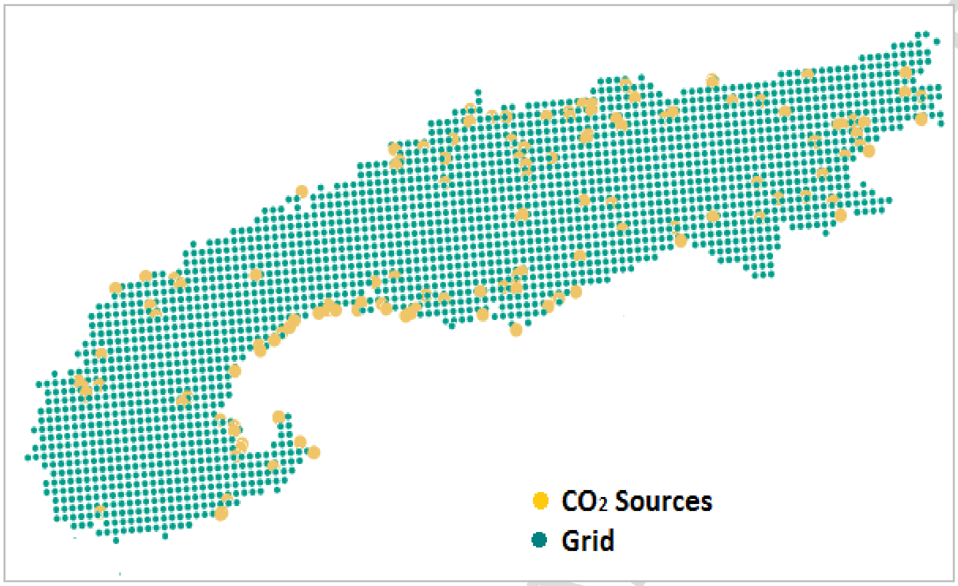

Figure 4. *Grid map of the identified CO_2 sources in the Alpine Region.*

4. Results and discussion

The results and discussions presented in this section are reflections of the 192 sampled hours and refer to the sets of prices for carbon and fossil fuels introduced in Table 1. All annual estimates are weighted according to the scheme described in Section 3.4.

4.1. Power generation mix

Figures 5−7 present the evolution of the resulting power generation mix at the sampled hours for all sets of carbon prices and FFPs described in Section 3. It should be noted that the contribution of base-load coal plants (which provide 10% of the demand in each region) and existing hydropower plants (which provide about 18% of the total demand of the entire region) remains constant in all the cases. Consequently, the variations in carbon price and fossil market values mainly affect the contribution of intermittent RES (in this case solar and wind energy) and, to a much lesser extent, the contribution of new hydropower and biomass plants.

For instance, at zero carbon price and base-case FFPs the power generation is dominated by natural gas with minor contributions from new hydropower (about 9%), biomass (1.3%) and wind energy (0.25%), Figure 5−S{0, 1}. When the carbon price was increased at an interval of 50 €/tonne CO_2, the share of intermittent RES (particularly solar) progressively increases to 17% of the power demand at a carbon price of 200 €/tonne CO_2 (Figure 5). On the other hand, when the FFPs are increased by 50 and 100% of their base case values and at zero carbon price, the contribution from solar gradually increases to 11% (Figure 6−S{0, 1.5}) and 16% (Figure 7−S{0, 2}) of the power demand, respectively. Furthermore, at FFPs 50% higher than the base case and zero carbon price the contribution of solar is fully used in the power grid (Figure 6-S{0, 1.5}), whereas at FFPs 100% higher than the base case, periods when generation exceeds demand start to appear even at zero carbon price (Figure 7-S{0, 2}). In all the cases the contribution of wind energy is relatively small.

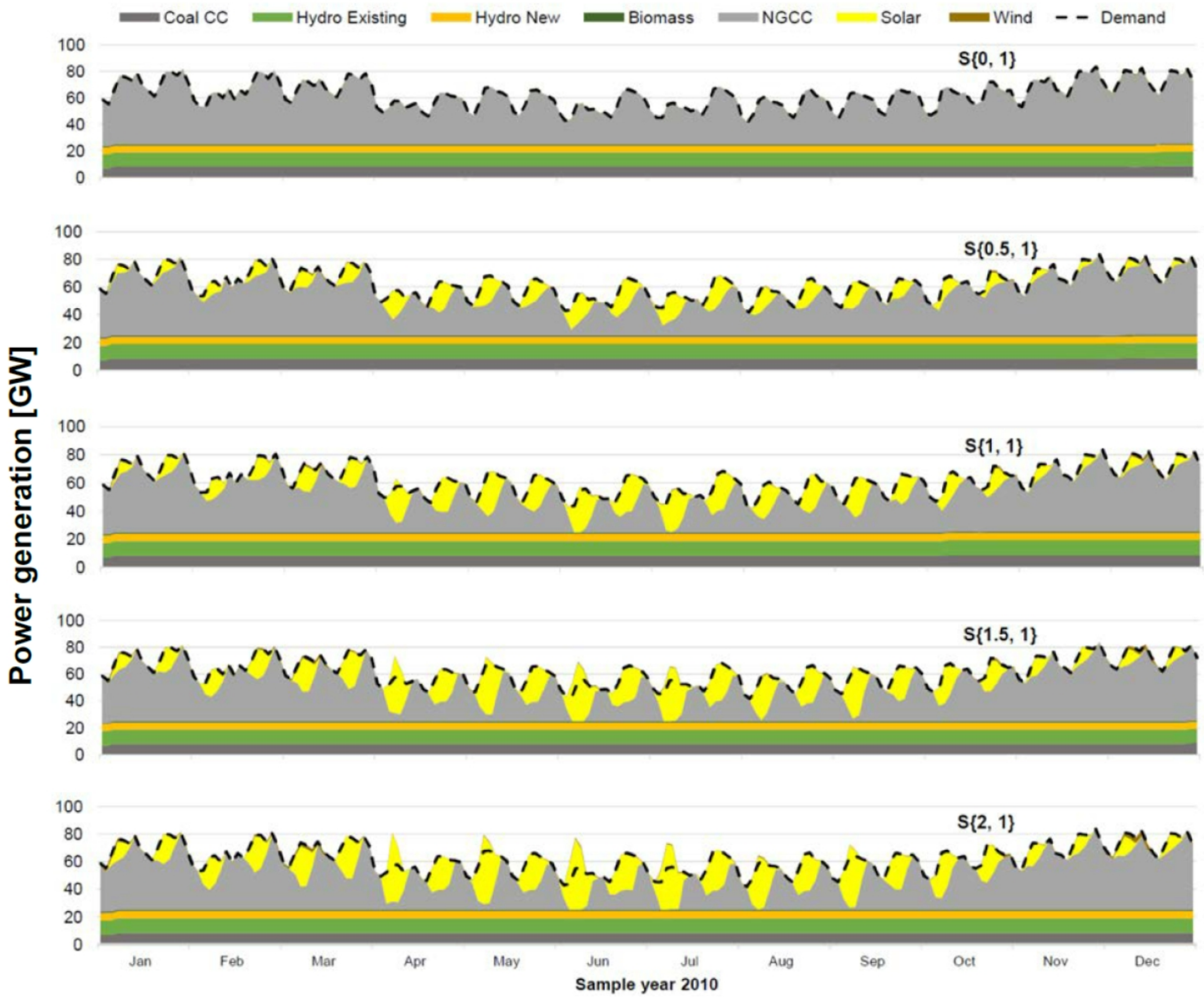

Figure 5. *Aggregated hourly power dispatch at the sampled hours for carbon prices in the range of 0−200 €/tonne and base case FFPs. Over-generation—the power available for PtG and PtL—is represented by the area above the demand.*

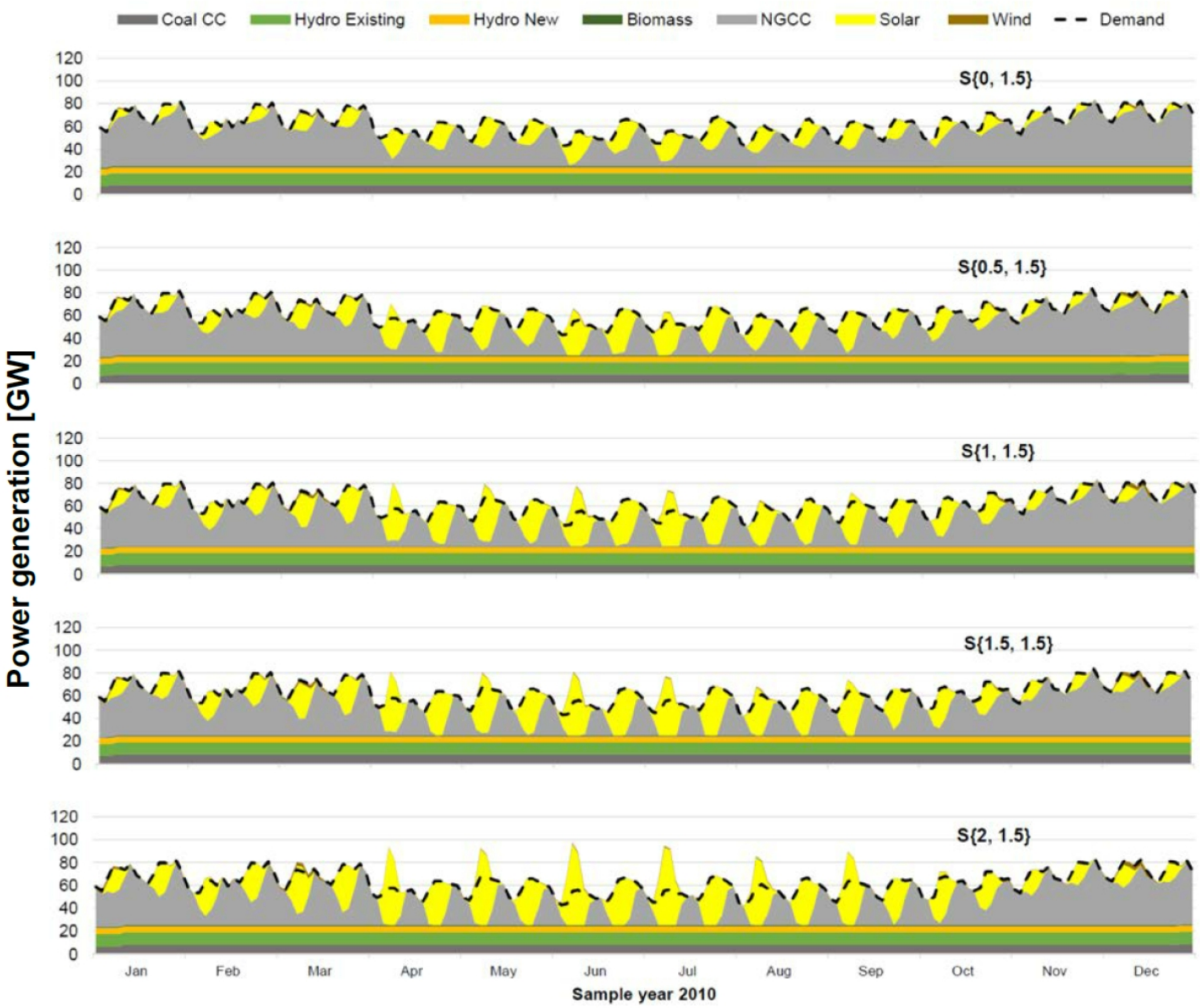

Figure 6. *Aggregated hourly power dispatch at the sampled hours for carbon prices in the range of 0−200 €/tonne and at medium FFPs. Over-generation—the power available for PtG and PtL—is represented by the area above the demand.*

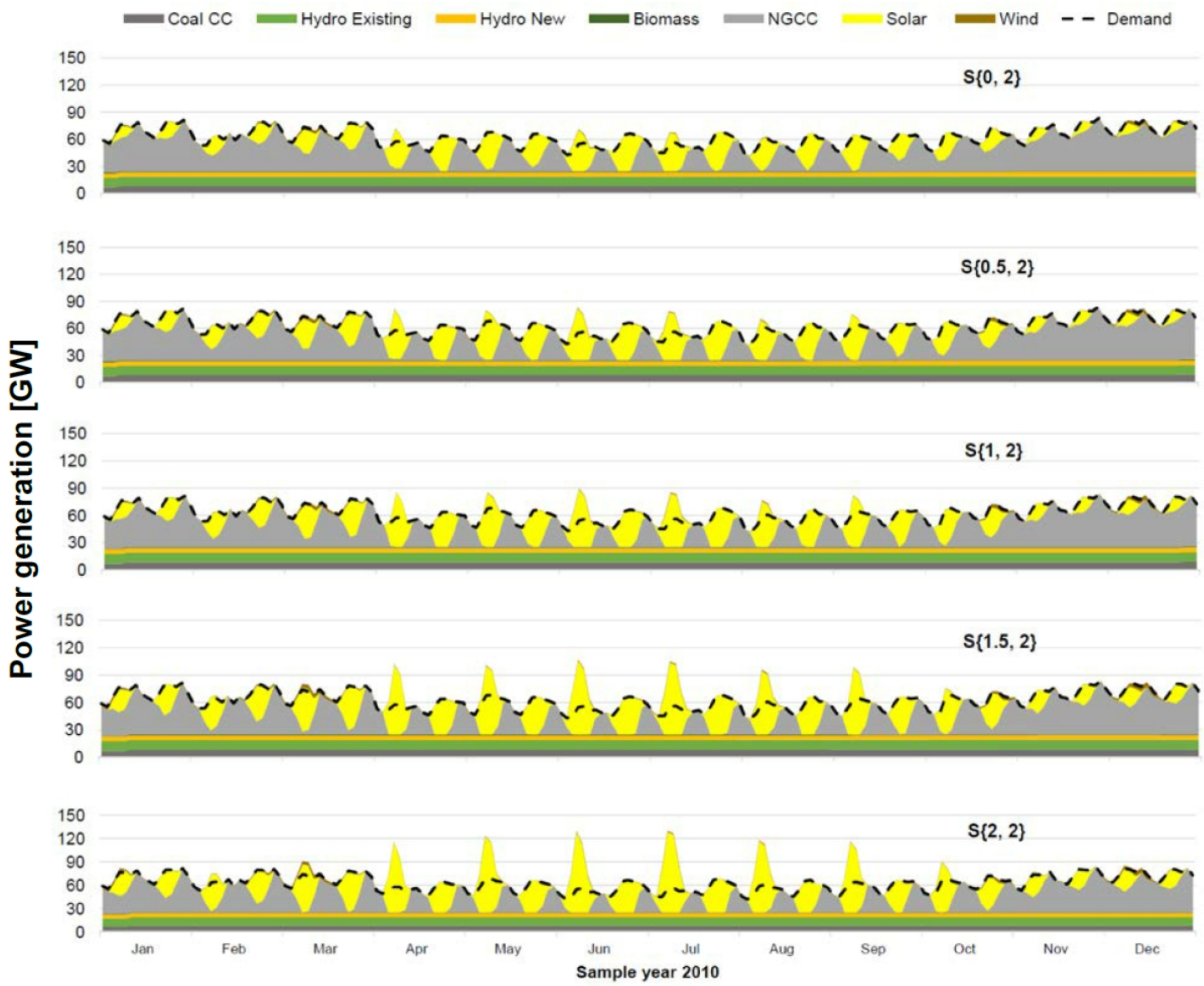

Figure 7. *Aggregated hourly power dispatch at the sampled hours for carbon prices in the range of 0−200 €/tonne and at high FFPs. Over-generation—the power available for PtG and PtL—is represented by the area above the demand.*

During the sample year, the total power demand was 530 TWh, of which—depending on the carbon and fossil prices—about 28–53% is met with RES and the remainder with fossil fuel, see Figure 8a. The low and high ends of the range correspond to scenarios S{0, 1} and S{2, 2}, respectively. Figure 8b shows the fraction of renewable power that is directly fed to the power grid, the remainder of the generated renewable power is either used for PtG/PtL or curtailed. Accordingly, the fraction decreases with increasing carbon price and FFPs. This behavior can be explained by the fact that at high carbon price and/or high FFPs the share of intermittent RES in the generation mix is high, which increases occurrences when supply exceeds demand.

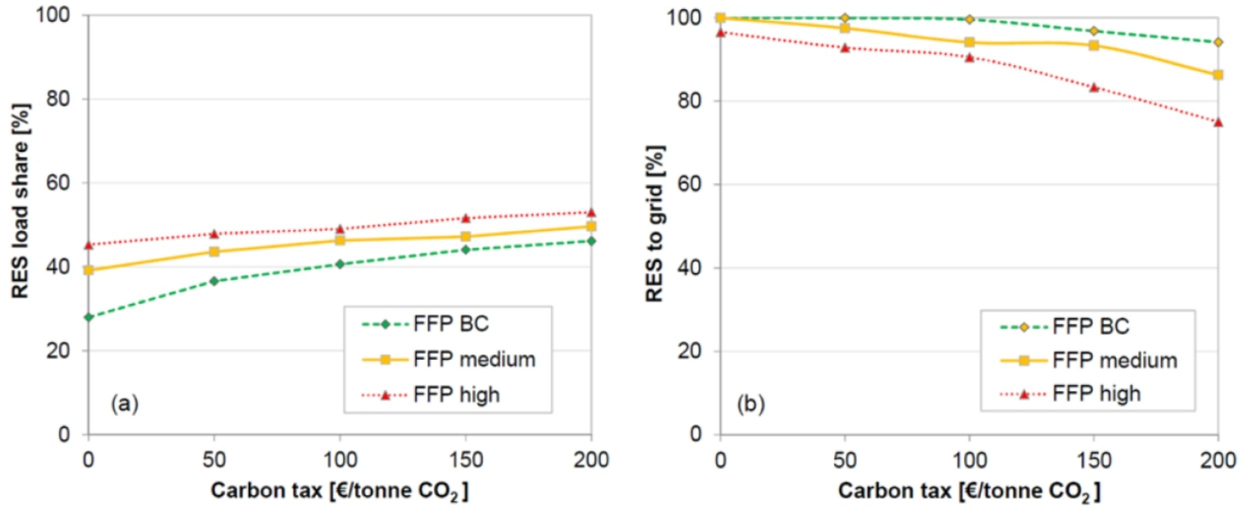

Figure 8. *The fraction of power generated from RES that is directly fed to power grid to satisfy demand, a, and its corresponding share of the total RES generation, b.*

4.2. Power transmissions

The model also uses existing transmission capacities among the regions studied. The transmission capacities are adopted from the European Network of Transmission System Operators (ENTSO-E). The net annual power transmissions for the investigated sets of carbon and fossil prices are presented in Figure 9. At a low carbon price and base case FFPs the contribution of intermittent renewables to the generation mix is insignificant and, therefore, the transmitted power is dominated by hydroelectric. At high carbon and fossil fuel prices, the contribution of intermittent electricity increases to 40% for S{2, 2}, of which about 60% is directly fed to the grid, reducing power transmissions, see Figure 9c. The reason for the shift in transmissions trend is due to the increase in solar power generation in net power importing regions, in this case Germany and Italy, as shown in Figure 9. It should be noted that the increase in solar generation reduces the magnitude of power transmissions as a result of the RES prioritzation constraints that ensure that investments on intermittent generation units are initiated only if there is a deficit in the power supply.

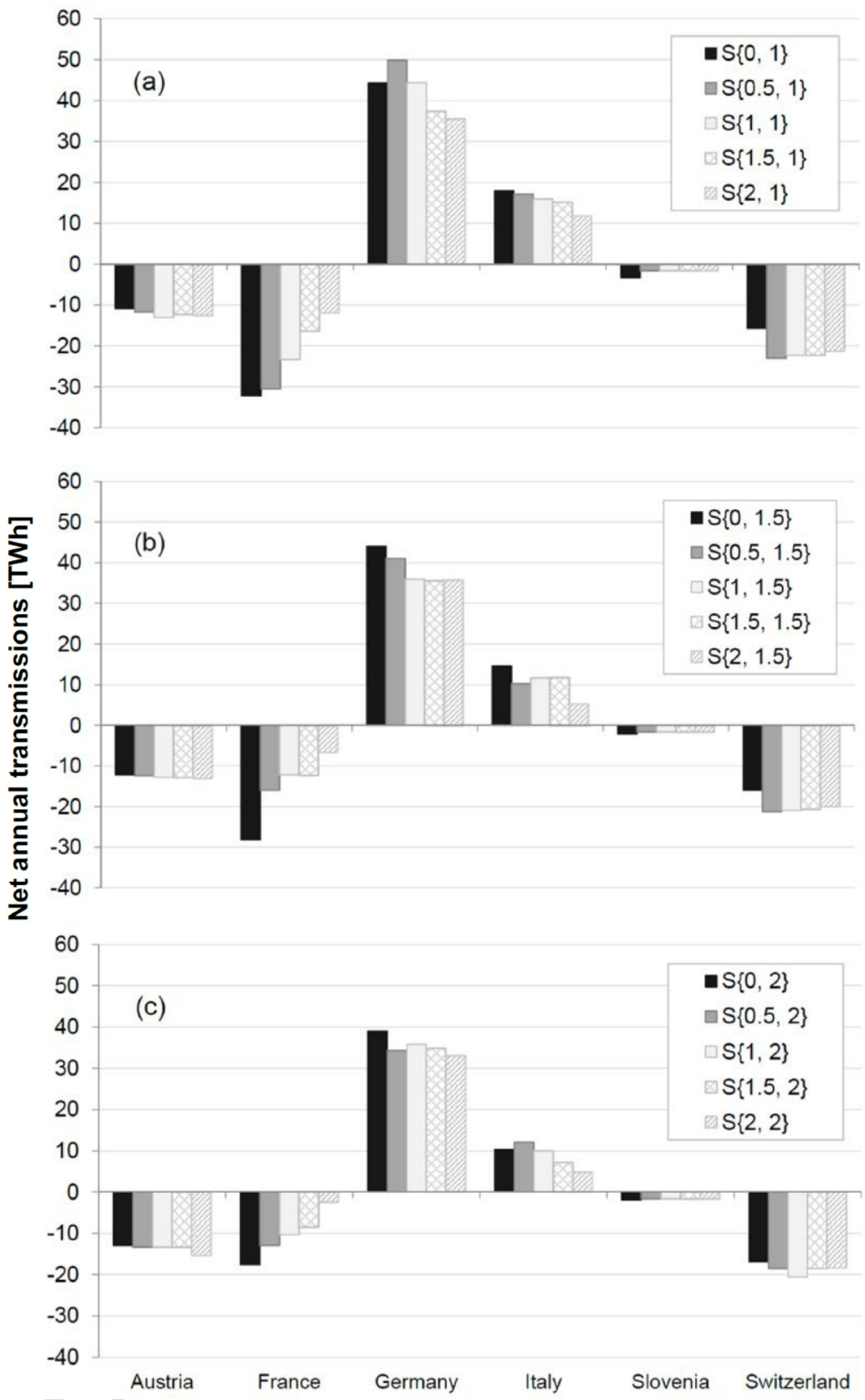

Figure 9. *Power transmissions among the regions over the range of carbon price 0–200€/tonne CO_2 and different levels of FFPs, base-case, a, medium, b, and high,c.*

4.3. Use of excess intermittent power in other sectors

The PtG and PtL technologies exploit excess intermittent power during periods when supply exceeds demand. In the sample year, an over-generation potential in the range of 0−65 GW is observed (see Figures 5−7) resulting in an annual total in the range of 0−93 TWh.

Figure 10a presents the corresponding amounts of methanol produced from the over-generated power in TWh/year. Accordingly, the model produces mainly methanol and traces of synthetic natural gas (SNG), particularly in the high end of the carbon price and FFPs ranges considered. This behavior is due to the fact that, in the model, methanol can only replace transportation fuel (gasoline) which generally has a higher market value than the gas fuels used in the heating sector. The PtG is linked to SNG production which can only replace fossil fuels in the heating sector.

The production of methanol is found to be rather more sensitive to variations in FFP than carbon price over the range of prices considered in this study. For instance, doubling the FFPs at 0 €/tonne CO_2 increases the share of intermittent renewables in the power supply mix from 0.25 to 19% and the production of methanol from 0 to 6 TWh/year. Whereas increasing the carbon price from 0 to 100 €/tonne CO_2 at the base case FFPs raises the share of intermittent renewables in the generation mix from 0.25 to 12.5% and methanol production from 0 to 0.6 TWh/year, see Figure 10a.

The potential for replacing gasoline transportation fuel with methanol produced in PtL technologies is shown in Figure 10b. Depending on the carbon price and FFPs, 1−11% of the gasoline use in transportation sector can be covered with methanol.

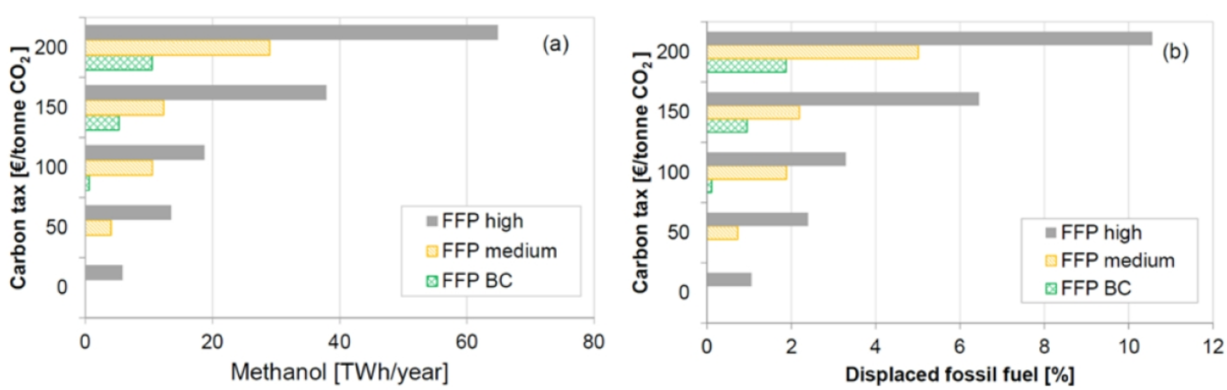

Figure 10. *Methanol produced, a, and the corresponding displacement of fossil fuels in transportation, b, over a range of carbon price 0-200€/tonne CO_2 and at different levels of FFPs*

4.4. Impact of RES penetration on CO_2 use and emissions

Another important aspect is that PtG and PtL provide the opportunity to recycle large volumes of captured CO_2 into the fuel supply system. Figure 11 shows the recycle rate of CO_2 by assuming a mole of CO_2 is consumed to produce a mole methanol or methane. In the range of carbon price and FFPs considered, 0.15−15 million tonnes of captured CO_2 is recycled. Recycling only affects the storage requirements for captured CO_2 [7], which could be crucial in countries where geological carbon storage is not permitted. In principle, by controlling the recycle rate to be equal to the amount of captured CO_2, the need for long-term storage can be avoided. CO_2 emissions from industrial processes are only delayed by one step before they finally are released. However, overall CO_2 emissions from the transportation and heating sectors are reduced because of displacement of fossil fuels.

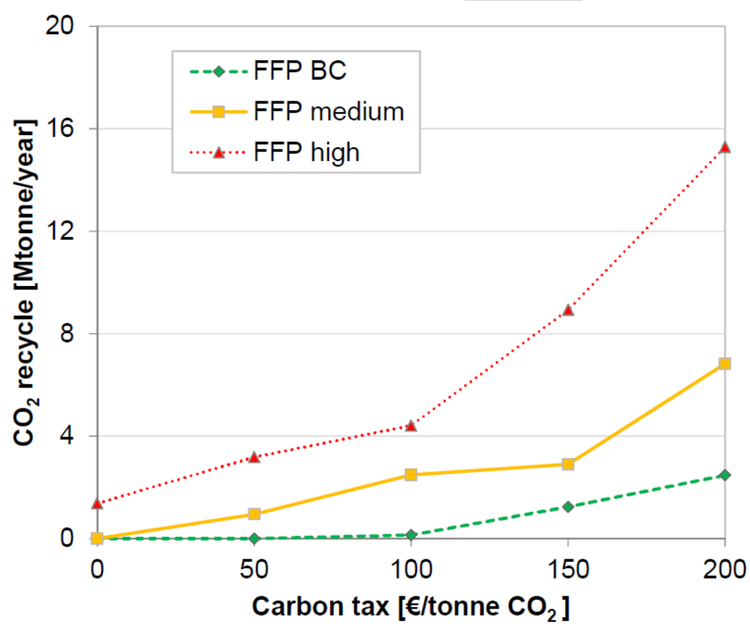

Figure 11. *CO_2 recycle [Million tonne/year], over the range of variation of carbon price and for the different levels of FFPs.*

PtG and PtL technologies decrease CO_2 emissions by enabling increased RES penetration, which displaces fossil fuels. As shown in Figure 8b, depending on the scenario, 75 to 99.9% of the RES-based power generation is directly transmitted to satisfy demand. Figure 12 shows the amount CO_2 emissions avoided because of direct substitution of fossil-based power with RES. As a result, depending on the scenario, 22−103 million tonnes of CO_2 emissions are avoided annually.

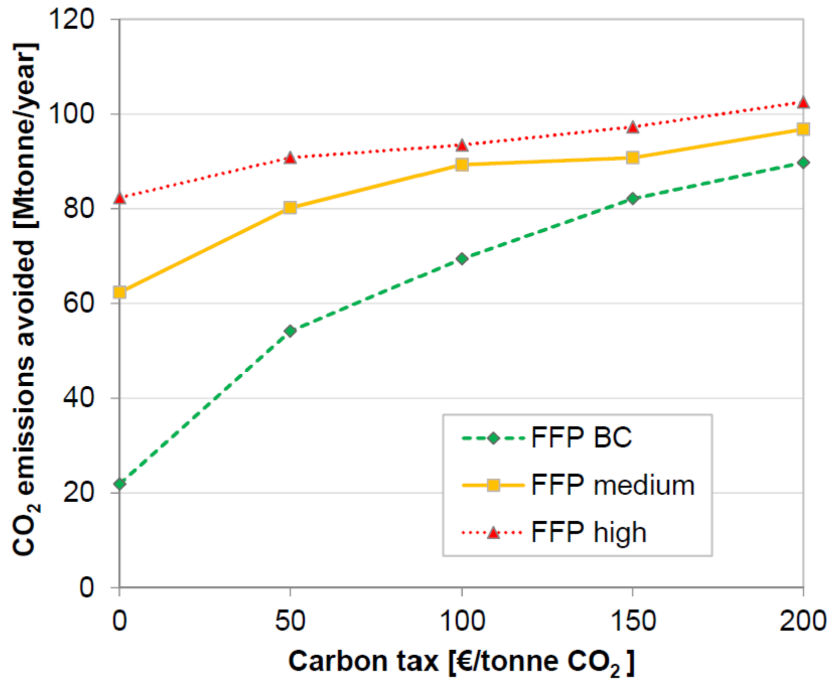

Figure 12. *CO_2 emissions avoided because of RES penetration in million tonnes per year, over the range of carbon price and FFPs.*

4.5. Curtailment and overgeneration

One impact of the PtG and PtL technologies on electricity systems is that curtailment is reduced. We assume that all excess electricity generation can be used for the production of gas and/or liquid should the model find it cost-effective to do so. In real energy systems, curtailment may also occur because of operational constraints on PtG and PtL. It may not be technically feasible to build PtG and PtL plants that operationally follow the peaks of the power generation profile, shown in Figures 5−7: however, electrochemical processes have fewer technical limitations than thermal conversion processes, such as minimum uptimes, minimum loadings and ramping constraints. Curtailment can also be minimized by coupling PtG and PtL with temporary power storages, such as batteries, in order to smooth out periods of peak power supply, but such operational details of the PtG and PtL are beyond the scope of this work.

Figure 13 shows the percentage of curtailment as a fraction of intermittent RES (solar and wind) for the sets of carbon and fossil fuels prices considered. Curtailment in this context refers to the surplus power because the model chose not to build PtG and/or PtL plants because of economic considerations. The weighting scheme by which the annual estimates are evaluated also adds bias, for instance, over-generation on a median day would be more likely to be converted into liquid or gas fuel than an equivalent over-generation on a peak day.

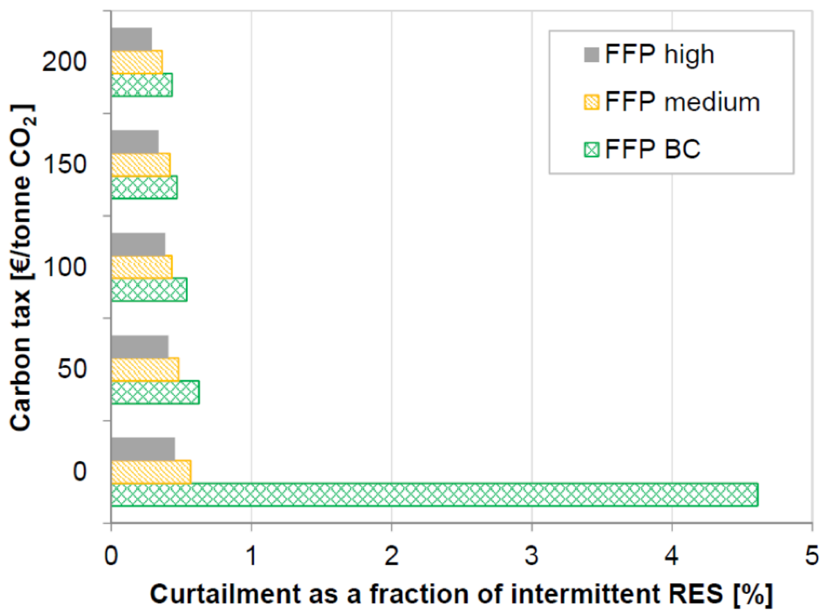

Figure 13. Curtailment as a fraction of intermittent RES

5. Conclusions

This study investigated the potential for integrating RES into the energy system of the Alpine region, emphasizing the quantification of power over-generation potentials as a result of large scale integration of RES. The results indicate a broad range of over-generation, from 0.85 to 65 GW, are possible for the capacities and economic conditions considered in this work.

We found that PtG and PtL add flexibility to the energy system by linking power to gas/liquid fuels that can be used in other sectors. This link is highly important because of the intermittency of RES electricity production. Over the range of prices assumed in this study, as much as 11% of gasoline in the transportation sector can be replaced with methanol produced from excess intermittent power.

In addition, PtG and PtL provide the opportunity to recycle large volumes of captured CO_2, as much as 15 million tonnes/year, into the fuel supply system. Furthermore, PtG and PtL enable deeper penetration of RES into the power sector. For instance, depending on carbon and fossil fuel prices, 22 to 103 million tonnes of CO_2 emissions can be avoided because of direct substitution of fossil fuel use with RES.

Under the assumed economic and operating conditions of the SOECs, these results indicate that PtG and PtL technologies can enable greater integration of renewables into the energy system. In particular, under global efforts to reduce CO_2 emissions, these technologies could play a crucial role in linking the electricity, heating, and transportation sectors, and providing long-term storage.

Acknowledgments

Part of the research was developed in the Young Scientists Summer Program at the International Institute for Systems Analysis (IIASA). Bio4Energy, a strategic research environment appointed by the Swedish government, Luleå University of Technology, the United States National Member Organization and the Swedish Research Council Formas (dnr. 942-2016-118 as well as travel grant), the IIASA Tropical Flagship Initiative (TFI), and the EC project S2Biom (grant number: 608622) are gratefully acknowledged for the financial support.

Nomenclature

BECCS	Bioenergy with carbon capture and sequestration
BC	Base case
bIGCC	biomass integrated gasification combined cycle
CHP	Combined heat and power plant
FFP	Fossil fuel price factor
RE	Renewable energy
RES	Renewable energy sources
SOEC	Solid oxide electrolysis cell
SNG	Substitute natural gas

PtG Power-to-gas

PtL Power-to-liquid

References

[1] E.S. Rubin, C. Chen, A.B. Rao, Cost and performance of fossil fuel power plants with CO2 capture and storage, Energy Policy. 35 (2007) 4444–4454. doi:10.1016/j.enpol.2007.03.009.

[2] D.L. Sanchez, J.H. Nelson, J. Johnston, A. Mileva, D.M. Kammen, Biomass enables the transition to a carbon-negative power system across western North America, Nat. Clim. Chang. (2015) 3–7. doi:10.1038/nclimate2488.

[3] N.R. McGlashan, M.H.W. Workman, B. Caldecott, N. Shah, Negative Emissions Technologies, Grantham Inst. Clim. Chang. Brief. Pap. No.8. (2012). https://workspace.imperial.ac.uk/climatechange/Public/pdfs/Briefing Papers/Briefing Paper 8.pdf.

[4] F. Kraxner, S. Nilsson, M. Obersteiner, Negative emissions from BioEnergy use, carbon capture and sequestration (BECS)—the case of biomass production by sustainable forest management from semi-natural temperate forests, Biomass and Bioenergy. 24 (2003) 285–296. doi:10.1016/S0961-9534(02)00172-1.

[5] Z. Zhan, W. Kobsiriphat, J.R. Wilson, M. Pillai, I. Kim, S. a. Barnett, Syngas Production By Coelectrolysis of CO 2 /H 2 O: The Basis for a Renewable Energy Cycle, Energy & Fuels. 23 (2009) 3089–3096. doi:10.1021/ef900111f.

[6] A. Varone, M. Ferrari, Power to liquid and power to gas: An option for the German Energiewende, Renew. Sustain. Energy Rev. 45 (2015) 207–218. doi:10.1016/j.rser.2015.01.049.

[7] J. Vandewalle, K. Bruninx, W. D'haeseleer, Effects of large-scale power to gas conversion on the power, gas and carbon sectors and their interactions, Energy Convers. Manag. 94 (2015) 28–39. doi:10.1016/j.enconman.2015.01.038.

[8] S. Schiebahn, T. Grube, M. Robinius, V. Tietze, B. Kumar, D. Stolten, Power to gas: Technological overview, systems analysis and economic assessment for a case study in Germany, Int. J.

Hydrogen Energy. 40 (2015) 4285–4294. doi:10.1016/j.ijhydene.2015.01.123.

[9] S.H. Jensen, X. Sun, S.D. Ebbesen, R. Knibbe, M. Mogensen, Hydrogen and synthetic fuel production using pressurized solid oxide electrolysis cells, Int. J. Hydrogen Energy. 35 (2010) 9544–9549. doi:10.1016/j.ijhydene.2010.06.065.

[10] H.S. De Boer, L. Grond, H. Moll, The application of power-to-gas , pumped hydro storage and compressed air energy storage in an electricity system at different wind power penetration levels, Energy. 72 (2014) 360–370. doi:10.1016/j.energy.2014.05.047.

[11] M. Jentsch, T. Trost, M. Sterner, Optimal use of Power-to-Gas energy storage systems in an 85% renewable energy scenario, Energy Procedia. 46 (2014) 254–261. doi:10.1016/j.egypro.2014.01.180.

[12] G. Gahleitner, Hydrogen from renewable electricity: An international review of power-to-gas pilot plants for stationary applications, Int. J. Hydrogen Energy. 38 (2013) 2039–2061. doi:10.1016/j.ijhydene.2012.12.010.

[13] Q. Fu, C. Mabilat, M. Zahid, A. Brisse, L. Gautier, Syngas production via high-temperature steam/CO2 co-electrolysis: an economic assessment, Energy Environ. Sci. 3 (2010) 1382. doi:10.1039/c0ee00092b.

[14] C. Graves, S.D. Ebbesen, M. Mogensen, K.S. Lackner, Sustainable hydrocarbon fuels by recycling CO2 and H2O with renewable or nuclear energy, Renew. Sustain. Energy Rev. 15 (2011) 1–23. doi:10.1016/j.rser.2010.07.014.

[15] I. Ridjan, B.V. Mathiesen, D. Connolly, N. Duić, The feasibility of synthetic fuels in renewable energy systems, Energy. 57 (2013) 76–84. doi:10.1016/j.energy.2013.01.046.

[16] W.L. Becker, R.J. Braun, M. Penev, M. Melaina, Production of Fischer-Tropsch liquid fuels from high temperature solid oxide co-electrolysis units, Energy. 47 (2012) 99–115. doi:10.1016/j.energy.2012.08.047.

[17] S.D. Ebbesen, M. Mogensen, Electrolysis of carbon dioxide in Solid Oxide Electrolysis Cells, J. Power Sources. 193 (2009) 349–358. doi:10.1016/j.jpowsour.2009.02.093.

[18] L. Chen, F. Chen, C. Xia, Direct synthesis of methane from CO2–H2O co-electrolysis in tubular solid

oxide electrolysis cells, Energy Environ. Sci. 7 (2014) 4018–4022. doi:10.1039/C4EE02786H.

[19] C. Gaudillere, L. Navarrete, J.M. Serra, Syngas production at intermediate temperature through H2O and CO2 electrolysis with a Cu-based solid oxide electrolyzer cell, Int. J. Hydrogen Energy. 39 (2014) 3047–3054. doi:10.1016/j.ijhydene.2013.12.045.

[20] E. Giglio, A. Lanzini, M. Santarelli, P. Leone, Synthetic natural gas via integrated high-temperature electrolysis and methanation: Part I—Energy performance, J. Energy Storage. 1 (2015) 22–37. doi:10.1016/j.est.2015.04.002.

[21] C. Graves, S.D. Ebbesen, M. Mogensen, Co-electrolysis of CO2 and H2O in solid oxide cells: Performance and durability, Solid State Ionics. 192 (2011) 398–403. doi:10.1016/j.ssi.2010.06.014.

[22] C.M. Stoots, High-Temperature Co- Electrolysis of H 2 O and CO 2 for Syngas Production, (2006) 2–6.

[23] C.M. Stoots, J.J. Hartvigsen, High-Temperature Co- Electrolysis of Steam and Carbon Dioxide for Direct Production of Syngas ; Equilibrium Model and Single-Cell Tests, (2007).

[24] G. Schiller, a. Ansar, M. Lang, O. Patz, High temperature water electrolysis using metal supported solid oxide electrolyser cells (SOEC), J. Appl. Electrochem. 39 (2009) 293–301. doi:10.1007/s10800-008-9672-6.

[25] Sunfire GmbH, Power to liquids. <http://www.sunfire.de/wp-content/uploads/BILit_FactSheet_POWER-TO-LIQUIDS_EMS_en.pdf>. Date acceced 2015.09.03, (n.d.). http://www.sunfire.de/wp-content/uploads/BILit_FactSheet_POWER-TO-LIQUIDS_EMS_en.pdf (accessed September 3, 2015).

[26] Sunfire GmbH, Power to gas. <http://www.sunfire.de/wp-content/uploads/BILit_FactSheet_POWER-TO-GAS_EMS_en.pdf>. Date acceced 2015.09.03, (n.d.). http://www.sunfire.de/wp-content/uploads/BILit_FactSheet_POWER-TO-GAS_EMS_en.pdf (accessed September 3, 2015).

[27] S. Leduc, E. Schmid, M. Obersteiner, K. Riahi, Methanol production by gasification using a geographically explicit model, Biomass and Bioenergy. 33 (2009) 745–751.

doi:10.1016/j.biombioe.2008.12.008.

[28] S. Leduc, D. Schwab, E. Dotzauer, E. Schmid, M. Obersteiner, Optimal location of wood gasification plants for methanol production with heat recovery, Int. J. Energy Res. 32 (2008) 1080–1091. doi:10.1002/er.1446.

[29] K. Natarajan, S. Leduc, P. Pelkonen, E. Tomppo, E. Dotzauer, Optimal Locations for Methanol and CHP Production in Eastern Finland, Bioenergy Res. 5 (2012) 412–423. doi:10.1007/s12155-011-9152-4.

[30] S. Leduc, E. Wetterlund, E. Dotzauer, G. Kindermann, CHP or biofuel production in Europe?, Energy Procedia. 20 (2012) 40–49. doi:10.1016/j.egypro.2012.03.006.

[31] E. Wetterlund, S. Leduc, E. Dotzauer, G. Kindermann, Optimal localisation of biofuel production on a European scale, Energy. 41 (2012) 462–472. doi:10.1016/j.energy.2012.02.051.

[32] J. Schmidt, S. Leduc, E. Dotzauer, E. Schmid, Cost-effective policy instruments for greenhouse gas emission reduction and fossil fuel substitution through bioenergy production in Austria, Energy Policy. 39 (2011) 3261–3280. doi:10.1016/j.enpol.2011.03.018.

[33] J. Schmidt, S. Leduc, E. Dotzauer, G. Kindermann, E. Schmid, Cost-effective CO2 emission reduction through heat, power and biofuel production from woody biomass: A spatially explicit comparison of conversion technologies, Appl. Energy. 87 (2010) 2128–2141. doi:10.1016/j.apenergy.2009.11.007.

[34] D. Khatiwada, S. Leduc, S. Silveira, I. Mccallum, Optimizing ethanol and bioelectricity production in sugarcane biore fi neries in Brazil, Renew. Energy. 85 (2016) 371–386. doi:10.1016/j.renene.2015.06.009.

[35] S. Leduc, F. Starfelt, E. Dotzauer, G. Kindermann, I. McCallum, M. Obersteiner, J. Lundgren, Optimal location of lignocellulosic ethanol refineries with polygeneration in Sweden, Energy. 35 (2010) 2709–2716. doi:10.1016/j.energy.2009.07.018.

[36] S. Leduc, K. Natarajan, E. Dotzauer, I. McCallum, M. Obersteiner, Optimizing biodiesel production in India, Appl. Energy. 86 (2009) S125–S131. doi:10.1016/j.apenergy.2009.05.024.

[37] E. Wetterlund, S. Leduc, E. Dotzauer, G. Kindermann, Optimal use of forest residues in Europe

under different policies—second generation biofuels versus combined heat and power, Biomass Convers. Biorefinery. (2012) 3–16. doi:10.1007/s13399-012-0054-2.

[38] C.T.M.T.M. Clack, Y. Xie, a. E.E. MacDonald, Linear programming techniques for developing an optimal electrical system including high-voltage direct-current transmission and storage, Int. J. Electr. Power Energy Syst. 68 (2015) 103–114. doi:10.1016/j.ijepes.2014.12.049.

[39] F. Kraxner, S. Leduc, H. Serrano Leon, J. Balest, G. Garegnani, G. Grilli, M. Ciolli, F. Ggeri, A. Paletto, A. Poljanec, C. Walzer, Recommendations and lessons learned for a renewable energy strategy in the Alps. recharge-green.eu, International Commission for the Protection of the Alps, Schaan, Liechtenstein, 2015.

[40] S. Leduc, J. Lundgren, O. Franklin, E. Dotzauer, Location of a biomass based methanol production plant: A dynamic problem in northern Sweden, Appl. Energy. 87 (2010) 68–75. doi:10.1016/j.apenergy.2009.02.009.

[41] S. Leduc, Development of an optimization model for the location of biofuel production plants, PhD Thesis, Luleå University of Technology, 2009. doi:ISBN 978-91-86233-48-8, ISSN 1402-1544.

[42] S. Fleck, S. Preis, L. Schulting, S. Schumutz, C. Trautwein, Save the Alpine Rivers Scientific foundations for identifying ecologically sensitive river stretches in the Alpine Arc, Vienna, Austria, 2013.

[43] Terrestrial Hydrology Group. Department of Civil and Environmental Engineering. Princeton University. Princeton. NJ 08544., Global Meteorological Forcing Dataset for land surface modeling. <http://hydrology.princeton.edu/data.pgf.php#>, (2007). http://hydrology.princeton.edu/data.pgf.php# (accessed June 30, 2015).

[44] Development of information base regarding potentials and the necessary technical, legal and socio-economic conditions for expanding wind energy in the Alpine space. <http://www.alpine-space.org/2000-2006/alpinewindharvest.html>, (2005). http://www.alpine-space.org/2000-2006/alpinewindharvest.html (accessed July 3, 2015).

[45] WINDATLAS UND WINDPOWTENTIALSTUDIE ÖSTERREICH. <http://www.windatlas.at/downloads/Endbericht.pdf>, (2011).

[46] J. Nelson, J. Johnston, A. Mileva, M. Fripp, I. Hoffman, A. Petros-Good, C. Blanco, D.M. Kammen, High-resolution modeling of the western North American power system demonstrates low-cost and low-carbon futures, Energy Policy. 43 (2012) 436–447. doi:10.1016/j.enpol.2012.01.031.

[47] M. Fripp, Optimal Investment in Wind and Solar Power in California, University of California, Berkeley. Doctoral Thesis, 2008.

[48] K.Z. House, a. C. Baclig, M. Ranjan, E. a. van Nierop, J. Wilcox, H.J. Herzog, Economic and energetic analysis of capturing CO2 from ambient air, Proc. Natl. Acad. Sci. 108 (2011) 20428–20433. doi:10.1073/pnas.1012253108.

[49] Center for Global Development, Carbon Monitoring for Action (CARMA). <http://www.carma.org>, (2007). http://www.carma.org (accessed February 3, 2015).

[50] Black & Veatch, Cost and Performance data for Power Generation Technologies, 2012.

[51] S.N. Uddin, L. Barreto, Biomass-fired cogeneration systems with CO2 capture and storage, Renew. Energy. 32 (2007) 1006–1019. doi:10.1016/j.renene.2006.04.009.

[52] a. Marbe, S. Harvey, T. Berntsson, Biofuel gasification combined heat and power - New implementation opportunities resulting from combined supply of process steam and district heating, Energy. 29 (2004) 1117–1137. doi:10.1016/j.energy.2004.01.005.

[53] V. Dornburg, a. P.C. Faaij, Efficiency and economy of wood-fired biomass energy systems in relation to scale regarding heat and power generation using combustion and gasification technologies, Biomass and Bioenergy. 21 (2001) 91–108. doi:10.1016/S0961-9534(01)00030-7.

[54] P. Börjesson, L. Gustavsson, Regional production and utilization of biomass in Sweden, Energy. 21 (1996) 747–764. doi:10.1016/0360-5442(96)00029-1.

Appendix A. Cost of technologies

The capital cost of building each type of technology is collected from different sources. Table A1 summarizes the parameters of the reference bIGCC technology considered. Costs of other plant capacities are scaled based on the reference plant using the power law of capacity with a scaling exponent of 0.7. Table A2 summarizes the cost of technologies and economic parameters used in relation to PtG, PtL, solar, wind and hydropower technologies. For consistency, capital cost estimates are based on future projections for the year 2020, (e.g., [6,11,50]). All cost data refer to Euro value of the first quarter of 2010, assuming currency conversion factor of 1.30 $/€. The investment costs are amortized over the operational life time of the respective technology by assuming 5% interest rate and 25 years of economic lifetime.

For hydropower and bioenergy systems the investment, operation and maintenance costs are pre-calculated based on resources potential in every demand area and supplied to the model as parameters. In the model, coal and natural gas are set to satisfy deficit in energy supply and the associated costs are accounted in terms of the energy carrier market value. Whereas for the rest of the technologies, estimation of capital and O&M costs are internalized in the model based on capacity factors and capacity limits.

Table A1. Input data for the reference bioenergy production technologies [51–53]. All costs are adjusted to $€_{2010}$ using Chemical Engineering Plant Cost Index (CEPCI) 2010. Efficiencies refer to the LHV of biomass on dry basis.

	bIGCC

Parameter	Unit	Tech1	Tech2
Maximum size	$t_{biomass}$/hour	6.35	33.88
Base plant capacity	MW	6	30
Base investment cost	M€/year	4.11	11.75
O&M cost	€/$GJ_{biomass}$	0.41	1.18
Heat efficiency	%	50	40
Power efficiency	%	35	45

Table A2. Biomass (refers to forest residue) transportation cost and related emissions. Energy conversions refer to 18.5 GJ/tonne, LHV dry basis, and 55% moisture content. Cost data are adjusted to €$_{2010}$.

Transport type	Transport cost[a]	Emissions[b]
	€/TJ/km	tCO_2/PJ/km
Truck	$307 + 6.92 \times d$	5.82
Train	$648 + 0.96 \times d$	2.97

[a]*Transportation costs are adapted from* [54]. *d is the transportation distance in km. The transportation cost values are for wet biomass (as received basis, 55% moisture content).*

[b]*Emission factors are taken from* [31].

Table A3. Cost of conversion technologies and economic parameters

Parameter	PtL	PtG	Solar	Wind	Hydropower	Unit
Capital cost	1000[a]	800[a]	3750[c]	1980[e]	4000–5000[f]	€/kW
Economic life time	25	25	25	25	25	years
O&M fixed	5[b]	5[b]	5.14[d]	6.84[d]	0.03–0.185[g]	
O&M variable			0	0	6[h]	€/MWh
Electricity	50	50				€/MWh
CO_2	20	20				€/tonne
Water	2	2				€/tonne

Conversion efficiency	70	70		%

[a]*Capital cost includes both the SOEC assembly as well as the synthesis plant from syngas to methanol in the case of PtL* [6] *and syngas to methane in the case of PtG* [7].

[b]*Fixed O&M cost as % of the corresponding capital cost* [6].

[c]*Non-tracking commercial solar PV technology with 4kW (DC) installed capacity is considered for this study. The capital, fixed O&M cost are adopted from* [50]. *The capital cost estimates are expected to have uncertainties of +25%.*

[d]*Fixed O&M cost for solar and wind technologies in €/MWh* [50].

[e]*Capital cost estimate reported here is for onshore wind turbines, with expected uncertainties of less than +25%* [50].

[f]*Capital cost of new hydropower systems are averaged ranges. In general, typical capital cost estimates vary between 4000−5000 €/kW depending on plant size. These values are averaged from maximum and minimum estimate ranges of 2500−10000 $/kW for plant sizes less than 1MW, 2000−7500 $/kW for plant sizes 1−10MW and 1750−6250 $/kW for plant sizes greater than 10MW. Capacity levelized capital cost estimate of 3500 $/kW (with uncertainties of +35%) is reported in literature* [50], *which lays within the above range.*

[g]*Total O&M cost (in €/GWh) for hydroelectric are averaged ranges. Depending on the size of the plant O&M cost can vary between 0.03−0.185 $/GWh. These values are averaged from maximum and minimum estimate ranges of 55−185 $/MWh for plant sizes less than 1MW, 45−120 $/MWh for plant sizes 1−10MW and 40−110 $/MWh for plant sizes greater than 10MW. Accordingly, the capital and O&M cost for every new hydropower installation is estimated beforehand based on the river catchment potential of each demand area and input to the model as parameters.*

[h]*Variable O&M for hydropower (€/MWh)* [50]. *Already included in the total O&M cost.*

Appendix B. Energy prices

The prices of energy, by sector and country, used in this study are summarized in Table B1 [31].

Table B1. Energy prices (€/GJ) used in this study [31]

Country	Heating	Transport	Power
Austria	8.5	11.9	21.1
France	6.8	12.0	13.6
Germany	7.9	12.3	21.1
Italy	9.5	13.9	22.5
Slovenia	5.1	12.0	20.0
Switzerland	6.8	11.3	21.1

Appendix C. CO_2 emission factors

Table C1. Emission intensities (kg-CO_2/GJ) for displaced fossil energy carriers [31]

Country	Heating	Transport	Power
Austria	86.2	78.1	87.3
France	72.1	78.1	39.3
Germany	88.2	78.1	200.8
Italy	70.6	78.1	200.8
Slovenia	98.6	78.1	158
Switzerland	76.9	78.1	32